Pergamon

0301-9322(95)00056-9

Int. J. Multiphase Flow Vol. 22, No. 1, pp. 133–155, 1996

0301-9322/96 $15.00 + 0.00

KINETIC THEORY APPROACH TO INTERPHASE PROCESSES†

T. YTREHUS and S. ØSTMO

Department of Applied Mechanics, Thermo- and Fluid Dynamics, The Norwegian Institute of Technology, 7034 Trondheim, Norway

(Received 27 October 1994; in revised form 27 June 1995)

Abstract—Using kinetic theory approach, the fluid- and thermodynamics aspects of a vapor next to its interphase surface is studied under conditions of arbitrarily strong interphase processes in single component systems. The physical domain considered is a boundary layer known as the Knudsen layer, a few molecular mean free paths thick, in which the vapor adapts to given external equilibrium conditions. It is shown that the limiting flow conditions in strong evaporation closely corresponds to the sonic state. Expressions for the mass transfer are derived both in the general and in the linear cases, and comparisons are made with the classical Hertz–Knudsen and Schrage formulae which are both shown to be incomplete. The vapor is found to be far from its saturated state, both at the interphase surface and at the border of the continuum region. The coupling between the Knudsen layer and this latter region is shown by an example of evaporation into a shear flow.

Key Words: evaporation, condensation, Knudsen layers

1. INTRODUCTION

Ever since the pioneering work of Hertz (1882) and Knudsen (1915) on the evaporation of liquid mercury into vacuum, it has been known that strong interphase processes require treatment from the standpoint of kinetic theory, due to molecular non-equilibrium effects in such systems. The case studied by these authors was extreme in the sense that the process took place in a low-density environment, but it has been established more recently, for instance by Kogan & Makashev (1971), Cipolla *et al.* (1973), Ytrehus (1977), Sone & Onishi (1978) and Aoki & Cercignani (1983), that non-equilibrium effects are equally important also at ordinary pressure levels, provided that we are dealing with single component or multicomponent volatile substances. The explanation for this circumstance is connected with the lack of inert background gas in such systems, that can provide a diffusional resistance to the vapor in front of the interphase surface. As a result of this, the vapor–gas may attain a considerable velocity normal to the surface, and important non-equilibrium effects, like temperature jumps across the phase surface and deviation from saturation in the vapor state, may occur; and, even more fundamentally, the mass flux formulae for the interphase process itself have to be derived from the molecular theory in such cases.

Some of the physical issues involved may be discussed with reference to figure 1, showing a plane interface between a dense (solid or liquid) phase and its own vapor: molecules are released, or evaporated, from the interface according to a certain distribution function f_e, usually taken to be a half-range Maxwellian in velocity space ξ, and depending upon parameters such as the temperature T_L at the dense-phase side of the surface and the corresponding vapor saturation density $\rho_e = \rho_{sat}(T_L)$. Another group of molecules represented through the *a priori* unknown distribution function f_i are impinging from the vapor space upon the surface, and a certain fraction of these is recondensed at the surface while the remaining part is reflected with the distribution function f_r back into the vapor, as indicated in the figure. At equilibrium, the flux of molecules leaving the interphase surface equals that of the impinging ones, and the net mass transport, and

†This paper was presented at the *7th Norway–Israel Symposium on Fluid Mechanics of Heterogeneous Systems*, Trondheim, June 1994.

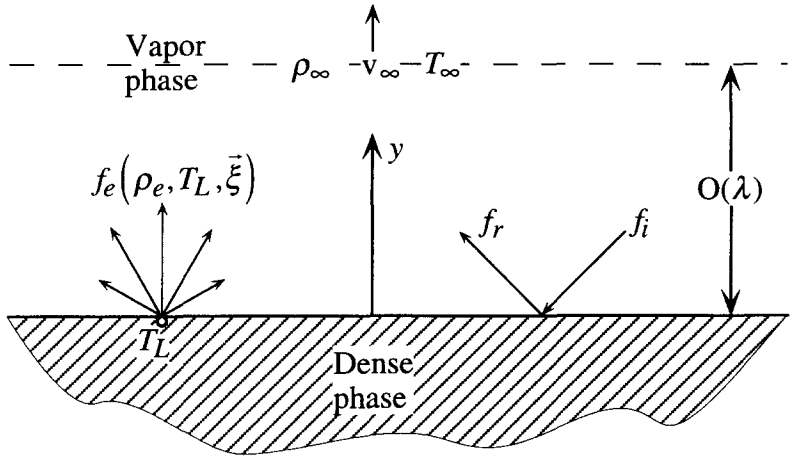

Figure 1. Definition sketch for evaporation Knudsen layer problem.

thereby the bulk velocity v_∞, becomes zero. The temperature becomes uniformly equal to T_L throughout the system, and the density in the vapor equals the saturation density $\rho_e = \rho_{sat}(T_L)$.

In general, however, the molecular fluxes to and from the surface are not equal, and this leads to a net mass transport and to a non-zero bulk velocity in the normal direction (figure 1). The temperatures associated with the two molecular streams (T_L and T_∞) may also be rather different, causing non-equilibrium effects to occur in a kinetic boundary layer of thickness of the order of the molecular mean free path λ in the vapor next to the surface; and the density and the pressure in the vapor are nowhere equal to their saturation values. Any fluid- and thermodynamic variable must in fact be computed from the dynamic laws that apply to transport phenomena on the mean free path scale in gases, and these are known to be contained in the classical Boltzmann equation of kinetic theory.

The total evaporated mass flux from the surface is easily computed in the case that f_e is a half-range Maxwellian in the velocity space. The result is

$$\dot{m}_e = \rho_e \sqrt{\frac{RT_L}{2\pi}} \qquad [1]$$

Now, Hertz (1882) and Knudsen (1915) reasoned that the impinging mass flux could be expressed in a similar way to an external Maxwellian f_∞ with parameters ρ_∞, v_∞ and T_∞, and, by neglecting the macroscopic vapor velocity v_∞, they arrived at the result

$$\dot{m}_i = \rho_\infty \sqrt{\frac{RT_\infty}{2\pi}} \qquad [2]$$

The net evaporated mass flux was therefore expressed as

$$\dot{m}_{HK} = \dot{m}_e - \dot{m}_i = \rho_e \sqrt{\frac{RT_L}{2\pi}} - \rho_\infty \sqrt{\frac{RT_\infty}{2\pi}}, \qquad [3]$$

which is now known as the classical Hertz–Knudsen formula. In spite of the approximate nature and of important theoretical shortcomings of the expression for $\dot{m}_i$, the formula is still in common use, partly due to its simplicity and partly due to lack of better knowledge. The formula was significantly improved by Schrage (1953), and by Kucherov & Rikenglas (1960), who took into account the vapor velocity v_∞ and thus included non-linear convective effects in the theory, without actually solving the governing gas–kinetic equations for the problem. This was done, although in a linear sense and for weak processes, by Patton & Springer (1969), Shankar & Marble (1971), Pao (1971), and by Cipolla *et al.* (1973) as mentioned above, and by Gajewski *et al.* (1974) for weakly non-linear cases. Then, Anisimov (1968) and Luikov *et al.* (1971) solved non-linear gas–kinetic

moment equations for the limiting case of strong evaporation at sonic conditions, and this approach was extended by Ytrehus (1977) to arbitrary strong evaporation, i.e. to cases with finite back-pressures, so as to also include the detailed structure of the expanding vapor layer from the interphase boundary and out into the equilibrium flow. Also, Monte Carlo simulations have been made of the non-linear evaporation condensation problem by Murakami & Oshima (1974), Kogan & Abramov (1991), Sibold & Urbassek (1993), and detailed numerical solutions of non-linear Boltzmann and BGK equations are given by, for instance, Yen (1973), Sone *et al.* (1990) and by Aoki *et al.* (1990).

For evaporation from the interphase surface the situation is largely as follows: for a given temperature T_L at the dense-phase side of the surface, and for a given corresponding vapor saturation pressure p_e (T_L), the process depends upon one additional free parameter; the ratio p_e/p_∞, where p_∞ is the external pressure. Other macroscopic quantities, like temperature, velocity and mass flux, are found to be unique functions of this one parameter. The gas–kinetic solution exhibits the length-scale of the molecular mean free path in the vapor, and this defines the vapor Knudsen layer adjacent to the surface. The solution exists for a parameter range $1 \leqslant p_e/p_\infty \leqslant (p_e/p_\infty)_{cr}$, where $(p_e/p_\infty)_{cr}$ corresponds to Mach number unity for the normal velocity component and has a value close to 4.81, depending slightly upon the specific solution method chosen. Below this value the velocity is subsonic and goes to zero as p_e/p_∞ goes to unity.

For net condensation onto the interphase surface the situation is less unique in the sense that two external parameters, for instance the pressure p_∞ and the temperature T_∞, may be prescribed, and the solution will thus depend upon both p_e/p_∞ and T_L/T_∞. According to how the external flow is generated, even supersonic states may occur, as discussed in particular by Sone *et al.* (1990), Kryukov (1991) and by Kogan & Abramov (1991). However, in the linear theory of weak condensation, the two-parameter aspect disappears, and in this regime condensation and evaporation become antisymmetric phenomena as would be expected on intuitive grounds. Still, outside of the Knudsen layers, in the continuum regime of flow, the two phenomena are highly asymmetrical, as was pointed out by Aoki & Cercignani (1983) and by Ytrehus & Aukrust (1986).

At present the results from kinetic theory for evaporation and condensation at planar surfaces are fairly complete and consistent for monatomic species, and some results are also available for polyatomic gases as given, for instance, by Cercignani (1981) and Frezzotti (1991). Mixtures have been treated by Ferron (1986), Onishi (1986) and by Frezzotti (1986), and an extension to dusty vapors has been given by Ytrehus & Stinessen (1991). Some results are also available for spheres (Edwards & Collins 1969; Onishi 1986; Sone & Sugimoto 1993) and for cylinders (Sugimoto & Sone 1992), and flows with evaporation in more complex geometries have been simulated by the Monte Carlo method by Nanbu (1986).

The longstanding and strong interest in the evaporation–condensation phenomena as is evident from this, by far not exhaustive review of literature on the subject, stems primarily from the fundamental aspects of the problems, but it has also been motivated by engineering applications such as vacuum distillation, vacuum vapor deposition, isotope separation and laser-pulse sputtering at surfaces. Also space applications, like outgassing from surfaces and its interaction with control and measurement equipment, have given some momentum to this research activity, along with even more exotic applications in astrophysics, like the formation and evolution of the dusty coma around active comets, e.g. Crifo (1986) and Ytrehus & Stinessen (1991).

In this paper we will review the moment solution of the Boltzmann equation for arbitrary strong evaporation, as originally given by Ytrehus (1977), and relate the results to the classical ones, in particular to those of Hertz–Knudsen and of Schrage as mentioned above. In so doing we shall linearize our results and develop formulae that can be readily used in conjunction with conventional macroscopic fluid dynamics. To show how coupling to continuum fluid mechanics actually works, we treat a specific example in which water is evaporated into a shear flow of its own vapor, resolving the macroscopic flow on the Navier–Stokes level, using a standard TEACH numerical code both for laminar and turbulent flow. Although not entirely new, this part of the study has not been published before, and it should therefore be of some original interest. We also discuss the thermodynamic state of the vapor and show that, in the case of water, the vapor is highly supersaturated as it enters the continuum shear flow. Although approximate in nature, the moment solution is known to produce fairly accurate results: within 5% of the values obtained for

macroscopic quantities by numerical BGK solutions and Monte Carlo simulations, as shown in a recent compilation of data by Sibold & Urbassek (1993). In addition, the method is simple and leads to a closed form solution for the microscopic structure of the flow, even for non-linear and critical flow conditions.

2. THE EVAPORATION KNUDSEN LAYER PROBLEM

2.1. General aspects

It is generally accepted that the fundamental Boltzmann equation of kinetic theory gives a realistic description of transport phenomena in gases down to the scale of the molecular mean free path. For structureless molecules, i.e. monatomic gases, the equation reads, in non-dimensional form and in the absence of external force fields (Chapman & Cowling 1952):

$$\mathrm{Kn}\left(\frac{\partial f}{\partial t} + \xi_j \frac{\partial f}{\partial x_j}\right) = \int (f'f_1' - ff_1) g b \mathrm{d}b \mathrm{d}\omega \mathrm{d}\xi_1 \qquad [4]$$

where $f(t, x, \xi)$ is the distribution function, ξ is molecular velocity and $g = |\xi - \xi_1|$ is the modulus of the relative velocity of molecules that collide with each other. b is the impact parameter in a binary collision, ω is the azimuthal angle and $f' = f(t, x, \xi')$, in which ξ' is a post-collision velocity. f_1 and f_1' are similarly defined for the collision partners. The only dimensionless parameter that occurs in [4] is the Knudsen number

$$\mathrm{Kn} = \frac{\lambda}{L} \qquad [5]$$

where λ is the molecular mean free path

$$\lambda \sim \frac{\eta}{\rho a}, \qquad [6]$$

and L is the length scale in the flow problem. Here, ρ is the mass density of the gas, η its viscosity and $a = \sqrt{\gamma RT}$ is the speed of sound.

It is well known that for small Knudsen numbers, i.e. for $\mathrm{Kn} \ll 1$, [4] can be expanded in powers of Kn around the local Maxwellian distribution function so that the conventional Navier–Stokes description is recovered at the first correction level. More importantly, this Chapman–Enskog procedure also gives the criteria for validity of the Navier–Stokes equations; these are

$$\mathrm{Kn}_g = \frac{\lambda}{L_g} \ll 1 \qquad [7]$$

where L_g is the smallest gradient-length in the flow; see for instance Chapman & Cowling (1952). It is, however, also well known that the convergence of the Chapman–Enskog expansion is non-uniform, and that it fails in singular layers next to the boundary, in which unbounded gradients may occur in the limit of $\mathrm{Kn} \to 0$, in the sense

$$\frac{\partial f}{\partial x_n} \sim \frac{1}{\mathrm{Kn}}, \qquad [8]$$

so that the full kinetic description, albeit one-dimensional, must be retained there. These are the Knudsen layers, for which the dimensional Boltzmann equation reads in steady cases

$$\xi_y \frac{\partial f}{\partial y} = \int (f'f_1' - ff_1) g b \mathrm{d}b \mathrm{d}\omega \mathrm{d}\xi_1, \qquad [9]$$

where the y-axis has been chosen as the coordinate normal to the boundary. This is why the Knudsen layer version of the Boltzmann equation is one-dimensional, and also why, in the general case, this version must retain the full non-linearity of the equation.

2.2. Boundary conditions

The dependent variable in the Boltzmann equation is the distribution function f, defined such that $f\mathrm{d}\xi$ gives the number of molecules per unit volume having velocities in the range $[\xi, \xi + \mathrm{d}\xi]$. Since [9] is of first order in the spatial variable y, one condition should be imposed at the boundary. In addition the function must be bounded at infinity. For evaporation at the boundary the usual conditions are

$$f(y = 0, \xi_y > 0) = a_w f_e + (1 - a_w) f_r \qquad [10]$$

$$f(y \to \infty, \xi) = f_\infty, \qquad [11]$$

where f_e is a Maxwellian based upon the temperature T_L at the dense-phase side of the boundary (figure 1) and upon the corresponding vapor saturation density $\rho_e = \rho_{sat}(T_L)$:

$$f_e = \frac{\rho_e/m}{(2\pi R T_L)^{3/2}} \exp\left(-\frac{\xi^2}{2RT_L}\right), \qquad [12]$$

and where f_∞ is a Maxwellian based upon the external flow variables:

$$f_\infty = \frac{\rho_\infty/m}{(2\pi R T_\infty)^{3/2}} \exp\left(-\frac{(\xi - \mathbf{u}_\infty)^2}{2RT_\infty}\right) \qquad [13]$$

Here, m is the mass of a molecule, R is the gas constant per unit mass and $\mathbf{u}_\infty = (0, v_\infty, 0)$ is the one-dimensional velocity vector at the outer edge of the Knudsen layer. f_r is a reflection of the *a priori* unknown distribution function f_i for molecules incident upon the surface and a_w is the so-called evaporation or condensation coefficient that takes values in the range [0, 1] depending upon the properties of the surface. Equation [10] means that only a fraction a_w of molecules in the state [12] are actually evaporated from the surface, and the same fraction a_w of incident molecules is recondensed into the surface. Therefore, the remaining fraction $(1 - a_w)$ of these latter molecules occurs in the reflection.

For simplicity we choose the conventional and most popular case of $a_w = 1$, and refer to Aoki *et al.* (1991) and Kogan (1992) for a discussion of the more general case with $a_w \neq 1$. Some effects of the non-unity evaporation–condensation coefficient are however considered in section 3.7 in the case of linear flow conditions.

Two points should be made at this stage: (i) although the distribution function for emission f_e is based upon the saturation density ρ_e, the vapor state at the boundary will not, in general, be saturated, due to the fact that [10] implies that only the half range $\xi_y > 0$ of the function should be applied, and the function f_i for impinging molecules does not correspond to the remaining half range $\xi_y \lesseqgtr 0$ of f_e as given in [12]; (ii) the external Maxwellian is based upon the fluid dynamics parameters ρ_∞, v_∞, T_∞ that are themselves an outcome of the evaporation process and that must be obtained with the solution. This Maxwellian state occurs at 'infinity' on the molecular mean free path scale λ, and corresponds to the Euler or Navier–Stokes level of fluid mechanics, as pointed out by Kogan & Makashev (1971). We assume that the external pressure is a known control parameter, and that it may be calculated from the equation of state

$$p_\infty = \rho_\infty R T_\infty \qquad [14]$$

along with the reference vapor pressure at the liquid temperature

$$p_e = \rho_e R T_L = \rho_{sat}(T_L) R T_L \qquad [15]$$

In addition it may be noted that, although the flowfield may also contain a velocity component along the surface, caused by driving terms other than evaporation, this effect is normally negligible within the Knudsen layer, since the shear boundary layer thickness δ is typically much larger than λ. We have, therefore, $\delta \sim L/\sqrt{\mathrm{Re}}$

$$\frac{\lambda}{\delta} \sim \frac{\lambda}{L}\sqrt{\mathrm{Re}} \sim \frac{M}{\sqrt{\mathrm{Re}}} \qquad [16]$$

where [6] has been used to derive the fundamental relation

$$\mathrm{Kn} \equiv \frac{\lambda}{L} \sim \frac{\mathrm{M}}{\mathrm{Re}}, \qquad [17]$$

$\mathrm{M} = U/a$ being the Mach number and $\mathrm{Re} = \rho UL/\eta$ being the Reynolds number for the flow along the surface. Therefore, the shear flow velocity at the edge of the Knudsen layer will be of the order

$$\Delta U_k \sim \frac{\partial U}{\partial y}\lambda \sim \frac{U}{\delta}\lambda \sim U\frac{\mathrm{M}}{\sqrt{\mathrm{Re}}} \qquad [18]$$

which is small compared to U under the normal flow conditions

$$\frac{\mathrm{M}}{\sqrt{\mathrm{Re}}} \ll 1 \qquad [19]$$

Equation [18] also gives the order of magnitude of an eventual slip velocity along the boundary, which again, by condition [19], is negligible in normal cases. This is the reason why only the normal velocity component v_∞ occurs in the external Maxwellian [13] and tangential flow and slip effects are absent in the boundary conditions.

2.3. The moment method

Instead of attempting a solution of [9] as it stands, a set of moment equations is generated by multiplying the equation by the velocity functions $\psi_\mu = (m, m\xi_y, -\frac{1}{2}m\xi^2, m\xi_y^2)$ for $\mu = 1, 2, 3, 4$, after an assumption is made for the form of the distribution function:

$$f(y,\xi) = a^+{}_e(y)f^+{}_e(\xi) + a^+{}_\infty(y)f^+{}_\infty(\xi) + a^-_\infty(y)f^-_\infty(\xi) \qquad [20]$$

Here, $f_e^+(\xi)$ is the $\xi_y > 0$ half-range of the function f_e given in [12], and $f_\infty^+(\xi)$ and $f_\infty^-(\xi)$ have similar definitions related to the function f_∞ in [13]. The $a(y)$s are amplitude functions to be determined, and their boundary conditions are derived from [10] and [11], with $a_w = 1$ as follows:

$$\begin{array}{rlrl} & a_e^+ = 1 & & a_e^+ = 0 \\ y = 0\text{:} & a_\infty^+ = 0 & y \to \infty\text{:} & a_\infty^+ = 1 \\ & a_\infty^- = \beta & & a_\infty^- = 1 \end{array} \qquad [21]$$

The boundary value $\beta = a_\infty^-(0)$ is an unknown parameter that must be obtained in the solution along with v_∞, T_∞ and ρ_∞. These four parameters then completely specify the flow conditions at the exit of the Knudsen layer (figure 1) and at the surface, since we have, by [10], [20] and [21],

$$f(y=0,\xi) = \begin{cases} f(y=0,\ \xi_y > 0) = f_e^+ \\ f(y=0,\ \xi_y < 0) = \beta f_\infty^- \end{cases} \qquad [22]$$

Macroscopic quantities are then computed in the standard way, i.e.

$$\rho = \int mf\underline{\mathrm{d}\xi}, \quad \rho v = \int m\xi_y f\underline{\mathrm{d}\xi} \qquad [23]$$

$$\frac{3}{2}\rho RT = \int \frac{1}{2}m(\xi - \mathbf{u})^2 f\underline{\mathrm{d}\xi},$$

where, in this case $\mathbf{u} = (0, v, 0)$.

The moment equations have the following basic form

$$\frac{\partial}{\partial y}\int \xi_y \psi_\mu f \underline{\mathrm{d}\xi} = 0, \quad \mu = 1,2,3 \tag{24a}$$

$$\frac{\partial}{\partial y}\int \xi_y \psi_4 f \underline{\mathrm{d}\xi} = \Delta Q[m\xi_y^2] \tag{24b}$$

where $\Delta Q[m\xi_y^2]$ is the contribution from the collision term of [9] when integrated with the weight function $m\xi_y^2$. For Maxwell molecules; i.e. molecules with inverse fifth-power repulsive interaction force, this collision term is expressed in closed form as (Vincenti & Kruger 1965)

$$\Delta Q[m\xi_y^2] = \frac{\pi}{\lambda_e}\sqrt{\frac{RT_L}{2\pi}}\,\frac{\rho}{\rho_e}\,\tau'_{yy}, \tag{25}$$

where τ'_{yy} is the viscous stress component

$$\tau'_{yy} = -m\left[\int (\xi_y - v)^2 f \underline{\mathrm{d}\xi} - \frac{1}{3}\int (\xi - \mathbf{u})^2 f \underline{\mathrm{d}\xi}\right], \tag{26}$$

and where λ_e is a reference mean free path defined as

$$\lambda_e = \frac{\eta_e(T_L)}{\rho_e}\sqrt{\frac{\pi}{2RT_L}}, \tag{27}$$

being a specific example within the general rule layed down in [6]. Here, $\eta_e(T_L)$ is the viscosity of the vapor in the emitting mode; i.e. at the saturated state corresponding to the temperature T_L of the dense-phase side of the interphase surface.

Equations [24] constitute a closed system for our problem when the Ansatz ([20]) for the distribution function f is taken into account. This means that the four equations are sufficient to determine the open parameters in the problem, i.e. ρ_∞, v_∞, T_∞ and the three amplitude functions $a_e^+(y)$, $a_\infty^+(y)$ and $a_\infty^-(y)$ in the expression [20].

The method would work for any molecular interaction law, but Maxwell molecules offer the simplest calculation. However, the interaction law will have an influence only upon the spatial structure of the flow, and not upon the above parameters (ρ_∞, v_∞, T_∞) that determine most quantities of practical interest, like for instance, the mass and heat fluxes in the process. To show this in more detail, we next proceed to a discussion of the conservation equations [24a], demonstrating their simple closed form solution in the general non-linear case.

2.4. Conservation equations

The three equations [24a] for $\mu = 1, 2, 3$ are the conservation equations, since the generating functions m, $m\xi_y$, $\frac{1}{2}m\xi^2$ are invariants during binary collisions and render the collision term ΔQ equal to zero. The equations are trivially integrated in the space variable y, and after the distribution function [20] is inserted and the half-range integrations in velocity space are performed, there results

$$\rho_e\sqrt{\frac{RT_L}{2\pi}}\,a_e^+(y) + \rho_\infty\sqrt{\frac{RT_\infty}{2\pi}}\,F^+ a_\infty^+(y) - \rho_\infty\sqrt{\frac{RT_\infty}{2\pi}}\,F^- a_\infty^-(y) = \rho_\infty v_\infty \tag{28a}$$

$$\frac{1}{2}\rho_e RT_L a_e^+(y) + \frac{1}{2}\rho_\infty RT_\infty G^+ a_\infty^+(y) + \frac{1}{2}\rho_\infty RT_\infty G^- a_\infty^-(y) = \rho_\infty v_\infty^2 + \rho_\infty RT_\infty \quad [28b]$$

$$2\rho_e RT_L\sqrt{\frac{RT_L}{2\pi}}\, a_e^+(y) + 2\rho_\infty RT_\infty\sqrt{\frac{RT_\infty}{2\pi}}\, H^+ a_\infty^+(y) - 2\rho_\infty RT_\infty\sqrt{\frac{RT_\infty}{2\pi}}\, H^- a_\infty^-(y)$$
$$= \rho_\infty v_\infty\left(\frac{1}{2}v_\infty^2 + \frac{5}{2}RT_\infty\right) \quad [28c]$$

The equations express the constant fluxes of mass, momentum and energy across the Knudsen layer, and in the right-hand sides these fluxes are evaluated at the external Maxwellian equilibrium state. The functions $F^\pm$, $G^\pm$ and $H^\pm$ are parameters that arise in the half-range integrations, and are defined in terms of the external speed ratio

$$S_\infty = \frac{v_\infty}{\sqrt{2RT_\infty}} \quad [29]$$

in the following way:

$$F^\pm = \sqrt{\pi}S_\infty(\pm 1 + \mathrm{erf}S_\infty) + \mathrm{e}^{-S_\infty^2} \quad [30a]$$

$$G^\pm = (2S_\infty^2 + 1)(1 \pm \mathrm{erf}S_\infty) \pm \frac{2}{\sqrt{\pi}}S_\infty \mathrm{e}^{-S_\infty^2} \quad [30b]$$

$$H^\pm = \frac{\sqrt{\pi}S_\infty}{2}\left(S_\infty^2 + \frac{5}{2}\right)(\pm 1 + \mathrm{erf}S_\infty) + \frac{1}{2}(S_\infty^2 + 2)\mathrm{e}^{-S_\infty^2} \quad [30c]$$

where $\mathrm{erf}S_\infty$ is the error function

$$\mathrm{erf}S_\infty = \frac{2}{\sqrt{\pi}}\int_0^{S_\infty} \mathrm{e}^{-x^2}\mathrm{d}x \quad [31]$$

In particular, at $y = 0$ and with [21] taken into account, the above system [28] is reduced to

$$\rho_e\sqrt{\frac{RT_L}{2\pi}} - \rho_\infty\sqrt{\frac{RT_\infty}{2\pi}}\,\beta F^- = \rho_\infty v_\infty \quad [32a]$$

$$\frac{1}{2}\rho_e RT_L + \frac{1}{2}\rho_\infty RT_\infty\,\beta G^- = \rho_\infty v_\infty^2 + \rho_\infty RT_\infty \quad [32b]$$

$$2\rho_e RT_L\sqrt{\frac{RT_L}{2\pi}} - 2\rho_\infty RT_\infty\sqrt{\frac{RT_\infty}{2\pi}}\,\beta H^- = \rho_\infty v_\infty\left(\frac{1}{2}v_\infty^2 + \frac{5}{2}RT_\infty\right) \quad [32c]$$

These equations relate the states at the interphase surface and external equilibrium in a similar way as the Rankine–Hugoniot equations relate the states upstream and downstream of a shock wave. The equations are solved for the three quantities S_∞, $\sqrt{T_\infty/T_L}$ and β in terms of the assumed known control parameter

$$z_e = \frac{p_e}{p_\infty} = \frac{\rho_e RT_L}{\rho_\infty RT_\infty}, \quad [33]$$

with the following result:

$$\sqrt{\frac{T_\infty}{T_L}} = -\frac{\sqrt{\pi}}{8} S_\infty + \sqrt{1 + \frac{\pi}{64} S_\infty^2} \quad [34a]$$

$$z_e = \frac{2e^{S_\infty^2}}{F^- + \sqrt{\frac{T_\infty}{T_L}} G^-} \quad [34b]$$

$$\beta = \frac{2(2S_\infty^2 + 1)\sqrt{\frac{T_\infty}{T_L}} - 2\sqrt{\pi} S_\infty}{F^- + \sqrt{\frac{T_\infty}{T_L}} G^-} \quad [34c]$$

For technical reasons S_∞ is considered known and z_e is considered unknown in these formulae. The results are summarized in table 1 below, in which also the quantity

$$\frac{\rho_\infty}{\rho_e} = \frac{1}{z_e T_\infty / T_L} \quad [35]$$

has been included to complete the external state.

From what is contained in the table, together with what was said in connection with [24] in the previous section, it is clear that most of the results of practical interest in the evaporation problem are already obtained at this 'Rankine–Hugoniot' level of analysis; and, like in the original Rankine–Hugoniot relations, the results are independent of gas properties related to intermolecular collision law, e.g. viscosity and heat conductivity.

2.5. Knudsen layer structure

Before [24b] is elaborated upon to give the detailed non-conserved moment equation, an important property of the system [28] is noted: [28] constitute a linear system for the three amplitude functions a_e^+, a_∞^+ and a_∞^-. With the 'Rankine–Huginot' relations [32] taken into account, the determinant of the system vanishes, so that two of the functions can be expressed in terms of the third, for example a_∞^-, as follows:

$$a_\infty^+(y) = \frac{a_\infty^-(y) - 1}{\beta - 1} \quad [36a]$$

$$a_\infty^+(y) = \frac{\beta - a_\infty^-(y)}{\beta - 1} \quad [36b]$$

Table 1. Gas dynamic parameters in evaporation

S_∞	p_e/p_∞	ρ_∞/ρ_e	T_∞/T_L	β	$\dot{m}/\dot{m}_e$
0.0	1.000	1.000	1.000	1.000	0.000
0.1	1.231	0.849	0.957	1.020	0.294
0.2	1.500	0.728	0.915	1.060	0.494
0.3	1.812	0.630	0.876	1.135	0.627
0.4	2.170	0.550	0.838	1.271	0.714
0.5	2.577	0.484	0.802	1.511	0.768
0.6	3.037	0.429	0.767	1.928	0.800
0.7	3.553	0.383	0.734	2.644	0.815
0.8	4.127	0.345	0.703	3.862	0.820
0.9	4.764	0.312	0.673	5.932	0.816
0.907†	4.813	0.310	0.671	6.132	0.816

†Critical value.

Then, [24b] can be worked out in terms of the one dependent variable, with the result

$$\frac{\mathrm{d}a_\infty^-}{\mathrm{d}y} = \frac{P}{\lambda_e}(a_\infty^- - 1)(a_\infty^- - r) \qquad [37]$$

where

$$P = \frac{\pi}{12}\frac{\rho_\infty}{\rho_e}(\beta - 1)\phi_1\phi_2/z_e\left(1 - \frac{T_\infty}{T_L}\right) \qquad [38a]$$

$$\phi_1 = \left(\frac{\rho_e}{\rho_\infty} - 2 + \beta(1 - \mathrm{erf}S_\infty)\right)\Big/(\beta - 1) \qquad [38b]$$

$$\phi_2 = (z_e - 2 + \beta(1 - \mathrm{erf}S_\infty))/(\beta - 1) \qquad [38c]$$

$$r = 1 - \frac{2}{\phi_1} + \frac{4S_\infty^2}{\phi_2} \qquad [38d]$$

Due to the solution of the conservation equations [32] as summarized in Table 1, it is clear that P and r in the above differential equations are both functions of one single parameter, S_∞, or $z_e = p_e/p_\infty$, that characterizes the actual flow conditions. Equation [37] must satisfy boundary and external conditions as given in [21], so that $a_\infty^-(0) = \beta$ and $a_\infty^+ \to 1$ as $y \to \infty$, where β takes values as contained in Table 1. Then, since $\beta > 1$ always, except in the case of no net mass transfer for which $S_\infty = 0$ and $\beta = 1$, [37] can give the correct approach to the external Maxwellian state $a_\infty^- = 1$ only as long as the parameter r in the right-hand side of the equation stays below, or at unity. Hence, we have the condition from [38d]:

$$\frac{2}{\phi_1(S_\infty)} - \frac{4S_\infty^2}{\phi_2(S_\infty)} \geq 0 \qquad [39]$$

This inequality is satisfied for values of S_∞ on the interval [0, 0.907], or, for the Mach number $\mathrm{M}_\infty = (6/5)^{1/2}S_\infty$ on the interval [0, 0.994]. This result suggests that the critical upper limit for the existence of the Knudsen layer solution is $\mathrm{M}_\infty = 1$. Our computed critical flow conditions are included in the lower line of Table 1.

The solution of [37] that gives the structure of the evaporation Knudsen layer is then as follows: for $r < 1$,

$$\frac{a_\infty^- - 1}{\beta - 1} = \left(\frac{a_\infty^- - r}{\beta - r}\right)\exp\left(-P(1 - r)\frac{y}{\lambda_e}\right) \qquad [40]$$

for $r = 1$,

$$\frac{a_\infty^- - 1}{\beta - 1} = \frac{1}{1 + P(\beta - 1)\dfrac{y}{\lambda_e}} \qquad [41]$$

With [36a] and [36b] the distribution function is then fully specified, and any macroscopic quantity of interest may be computed from defining relations like in [23], for instance density and temperature:

$$\frac{\rho}{\rho_\infty} = [a_\infty^-(y) - 1]\frac{1}{2}\phi_1 + 1 \qquad [42]$$

$$\frac{T}{T_\infty} = \frac{1}{3}\frac{\rho_\infty}{\rho}\left[3S_\infty^2 + 3 + (a_\infty^-(y) - 1)\phi_2 - 2S_\infty^2\frac{\rho_\infty}{\rho}\right] \qquad [43]$$

Numerical values of parameters required to define the Knudsen layer structure are contained in table 2.

Table 2. Kinetic parameters in evaporation

S_∞	r	P	ϕ_1	ϕ_2	$M_\infty = (6/5)^{1/2}S_\infty$
0.0	0.617	0.000	5.216	8.589	0.000
0.1	0.525	0.047	4.162	6.853	0.110
0.2	0.422	0.096	3.293	5.423	0.219
0.3	0.310	0.146	2.583	4.254	0.329
0.4	0.197	0.200	2.008	3.306	0.438
0.5	0.099	0.255	1.546	2.545	0.548
0.6	0.045	0.313	1.178	1.940	0.657
0.7	0.089	0.373	0.888	1.463	0.767
0.8	0.328	0.436	0.663	1.091	0.876
0.9	0.934	0.501	0.489	0.805	0.986
0.907†	1.000	0.506	0.478	0.786	0.994

†Critical value.

3. RESULTS AND DISCUSSION

3.1. General non-linear results

A fundamental finding in the present moment approach is the coupling of the external fluid dynamics variables to the interphase control parameters, T_L and $\rho_e = \rho_{sat}(T_L)$, in the gas-kinetic connection problem through the Knudsen layer, as expressed in [32a–c] and summarized in table 1. The dependence of a typical variable, $S_\infty = v_\infty/\sqrt{2RT_\infty}$, upon the one single driving parameter $z_e = p_e/p_\infty = \rho_e RT_L/\rho_\infty RT_\infty$, is exhibited in figure 2, where a comparison is made with numerical simulations of the full Boltzmann and Krook equations by Yen (1973) for a variety of flow conditions. Also included in the figure are experimental points obtained from a kinetically similar, but physically different system of flow from a thin perforated plate as described by Ytrehus *et al.* (1977). In these experiments the flow was created by molecular effusion from each individual of a large number (typically 10^5 m^{-2}) of perforations in a thin screen, such that the molecular boundary conditions [12] were realized in an average sense, but with a different definition of the density ρ_e. The measurements were made by free-molecular orifice probes in a conventional low density wind tunnel. These results constituted the first proof of the one-parameter aspect of the flow conditions in the evaporation–effusion problem.

Figure 3 shows the structure of the Knudsen layer in strong evaporation. Here the density from [38], and its inverse, the velocity, are plotted on the invariant scale

$$\ell = \frac{\lambda_e}{P(1-r)} \qquad [44]$$

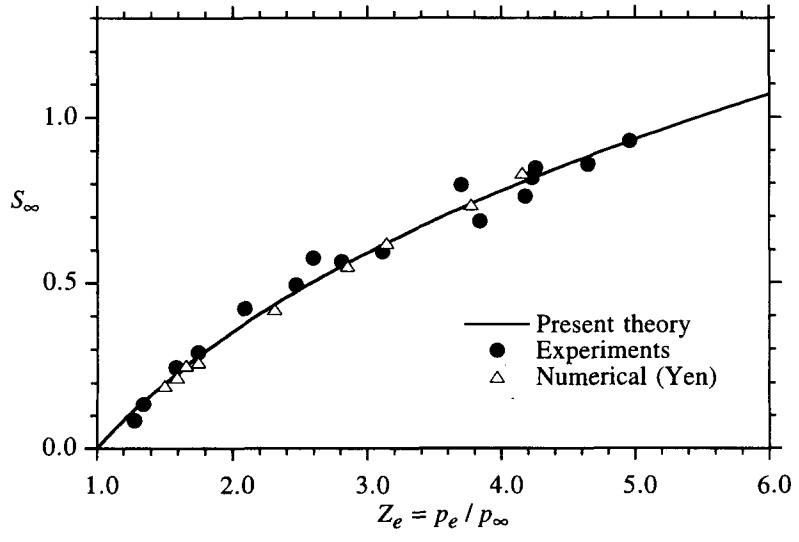

Figure 2. Downstream speed ratio vs pressure parameter $z_e = p_e/p_\infty$ in non-linear evaporation.

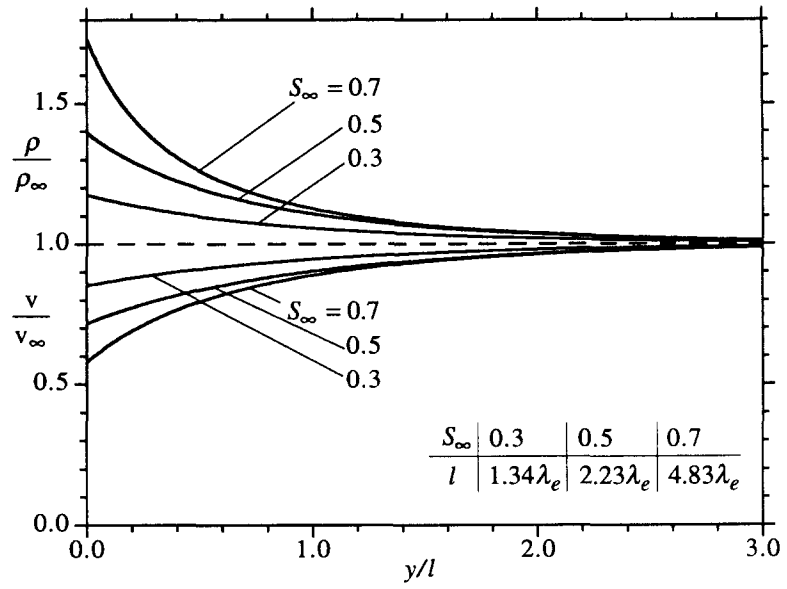

Figure 3. Knudsen layer structure at typical non-linear flow conditions.

as suggested in the solution [40]. The plot reveals an expanding vapor flow from the boundary. We note that, in the typical non-linear case, $S_\infty = 0.5$, we have for the density at $y = 0$, the vapor side of the interphase surface, $\rho(0)/\rho_\infty \simeq 1.4$, and from table 1 this is transformed into $\rho(0)/\rho_e \simeq 0.67$. This means that the density at the vapor side is only about 2/3 of the saturation value corresponding to the temperature T_L at the dense-phase side.

Now let us consider the temperature. From [43] and table 1 we obtain, in the case of $S_\infty = 0.5$, a vapor temperature at the surface $T(0)/T_L \simeq 0.85$. As will be discussed in section 3.4, this result implies that vapors of most common substances will be highly supersaturated as they leave the interphase boundary.

The temperature profile in the Knudsen layer at critical flow conditions; i.e. for $M_\infty = 1$, is furthermore shown in figure 4 in comparison with the experimental results of Mager *et al.* (1989). These experiments were made by evaporating iodine into a low-density environment, and measuring the temperature in the vapor flow by means of fluorescence spectroscopy. The results confirm the existence of a jump in the temperature from T_L at the dense-phase side to $T(0) \simeq 0.8T_L$ at the vapor side of the interphase boundary. This is an important first-order effect on boundary

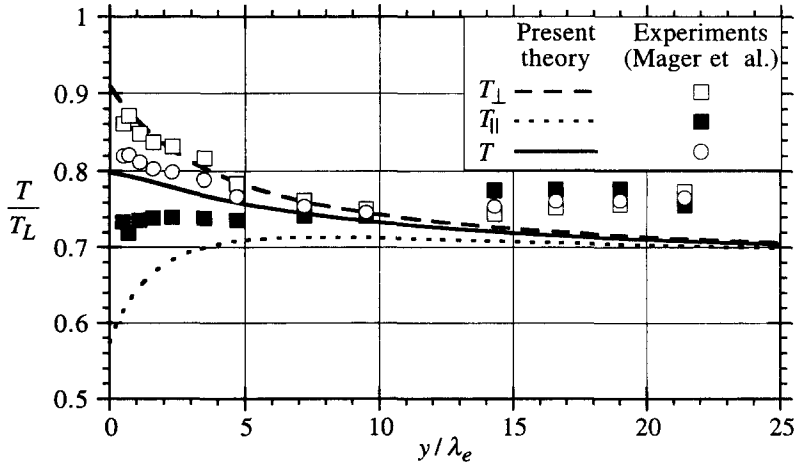

Figure 4. Temperature profiles in Knudsen layer at critical flow conditions.

values that cannot be captured in continuum theory treatments of the evaporation problem. Also shown in figure 4 are the parallel and perpendicular temperatures, defined as

$$\left.\begin{aligned} \tfrac{1}{2}\rho RT_{\parallel} &= \int \tfrac{1}{2} m C_{\parallel}^2 f \mathrm{d}\underline{\xi} \\ \rho RT_{\perp} &= \int \tfrac{1}{2} m C_{\perp}^2 f \mathrm{d}\underline{\xi} \end{aligned}\right\} \qquad [45]$$

where in general $C^2 = (\xi - \mathbf{u})^2$. Again there is good agreement between theory and experiments close to the boundary for the quantity $T_{\perp}$, whereas a marked discrepancy between the two is apparent for the quantity $T_{\parallel}$. The thickness of the vapor Knudsen layer in general follows from the scale ℓ defined by [44]. From table 2 it is quickly inferred that ℓ varies from about $3/4\lambda_e$ to several times this value as the evaporation increases from very weak, $S_\infty \ll 1$, to near critical $S_\infty = 0.907$. At critical conditions the solution [41] must be used, which yields the scale

$$\ell_{cr} = \frac{\lambda_e}{[P(\beta - 1)]_{cr.}} \simeq 2\lambda_e \qquad [46]$$

However, since the approach to equilibrium in this solution is algebraic rather than exponential, a length of the order of $10\ \ell_{cr} \simeq 20\ \lambda_e$ is required for the relaxation to be completed. This result has been confirmed in a recent Monte Carlo simulation by Sibold & Urbassek (1993).

The general non-linear theory predicts that the vapor Knudsen layer can expand only until the sonic value $M_\infty = 1$ is reached. From table 1 this corresponds to: $p_e/p_\infty \simeq 4.81$, $\rho_\infty/\rho_e \simeq 0.310$, $T_\infty/T_L \simeq 0.671$. If the external pressure is further reduced, i.e. to below about $1/5\ p_e$ so that p_e/p_∞ exceeds the critical value 4.81, the remaining expansion must occur outside in the continuum flow.

3.2. Relations to Schrage and Hertz–Knudsen formulae

The net evaporated mass flux follows directly from the conservation equation [32a] and reads

$$\dot{m} = \rho_e \sqrt{\frac{RT_L}{2\pi}} - \rho_\infty \sqrt{\frac{RT_\infty}{2\pi}}\, \beta F^-(S_\infty) \qquad [47]$$

Here $F^-(S_\infty)$ is the function of dimensionless velocity S_∞ given in [30a] and β is the boundary value relating to the mode incident upon the surface, e.g. [20], [21], [22]. The parameter β may be interpreted as a non-equilibrium backscattering factor, since $\beta = 1$ would correspond to pure streaming back into the surface by the half Maxwellian f_∞^-. Indeed, from table 1 we see that, at close to equilibrium conditions, $S_\infty \ll 1$, we have $\beta \simeq 1$, whereas in the critical state at strong evaporation we have $\beta \simeq 6$. At critical flow conditions the net backflow-effect amounts to about 18% of the emitted flux $\dot{m}_e$, introduced in [1] and defined as

$$\dot{m}_e = \int_{\xi_y > 0} \xi_y f_e \mathrm{d}\underline{\xi} = \rho_e \sqrt{\frac{RT_L}{2\pi}}, \qquad [48]$$

and β is thus seen to multiply a small number (≈ 0.03) in the normalized quantity m/m_e.

The Schrage formula for the evaporated mass flux appears to differ from the expression [47] by the lack of the factor β only, i.e. by Schrage (1953):

$$\dot{m}_S = \rho_e \sqrt{\frac{RT_L}{2\pi}} - \rho_\infty \sqrt{\frac{RT_\infty}{2\pi}}\, F^-(S_\infty) \qquad [49]$$

This would not make a very serious variance with the expression [47]—if the external flow variables ρ_∞, T_∞ and S_∞ were locked to the boundary values ρ_e and T_L by the Rankine–Huginot-like gas kinetic connection problem as specified in section 2.4. Then the comparison would be as in figure 5, in which values for ρ_∞/ρ_e and T_∞/T_L are taken from table 1. However, the problem with

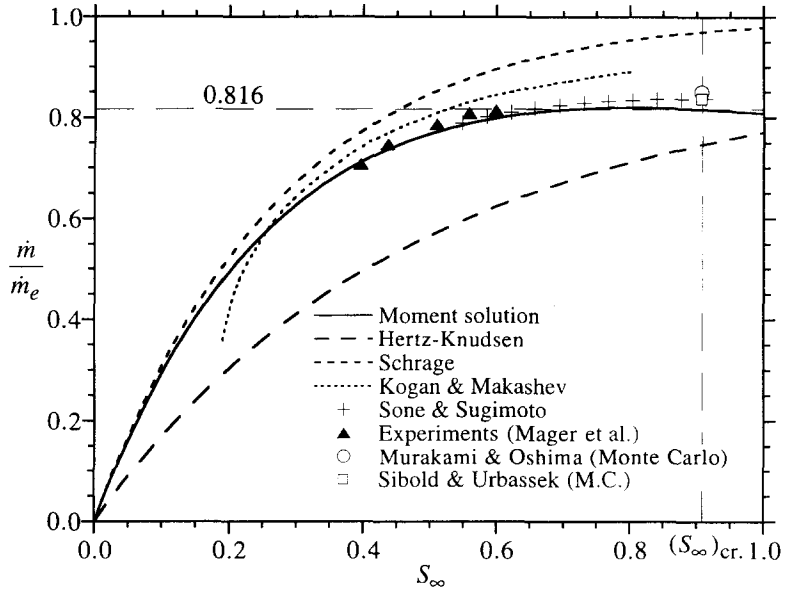

Figure 5. Normalized mass flux vs external speed ratio according to different approaches.

the Schrage formulation is that it fails to give the coupling between the external Maxwellian state and the physical control parameters T_L and $\rho_e = \rho_{sat}(T_L)$, so that values for ρ_∞ and T_∞ must be obtained from outside the Schrage theory itself.

Similar statements can also be made about the Hertz–Knudsen formula [3]

$$\dot{m}_{HK} = \rho_e \sqrt{\frac{RT_L}{2\pi}} - \rho_\infty \sqrt{\frac{RT_\infty}{2\pi}},$$

which neglects the whole bulk velocity effect in the external flow. Even so, the formula would give reasonable estimates for the mass flux—if proper values for ρ_∞ and T_∞ are provided from table 1, as shown in figure 5. The relative deviation from the more complete theory is, interestingly enough, larger at the medium and lower evaporation rates.

Both the Hertz–Knudsen and the Schrage formulae are classical results for interphase transport phenomena, and both formulae are based on sound physical reasoning, the latter being a more refined version of the first. But neither of these approaches realize the fundamental fact that only one of the external flow variables is free of choice, and that the other two follow from the gas kinetic connection problem across the Knudsen layer.

In figure 5 are further results from Monte Carlo simulations by Murakami & Oshima (1974), Sibold & Urbassek (1993), numerical BGK solutions by Kogan & Makashev (1971) and experimental results of Mager *et al.* (1989). Recent results from numerical solutions of the BGK equation from Sone & Sugimoto (1993) have also been included in the plot, and their deviation from the solid line of the moment method is visible on the drawing only near the limit of sonic flow conditions.

3.3. Linearized results

The non-linear cases of strong evaporation are extreme in the sense that they require substantial energy sources, either by radiation from outside or by thermal energy storage in the dense phase, in order to be realized. In many situations of practical interest the evaporation is weaker, and the theoretical results may be linearized into simple formulae. Under conditions such that

$$S_\infty \ll 1 \qquad [50]$$

we have from the systems [30a]–[30c] and [32a]–[32c], with errors of the order of S_∞^2:

$$\left.\begin{aligned} \Delta z_e &= \left(\frac{2}{\sqrt{\pi}} + \frac{9\sqrt{\pi}}{16}\right)S_\infty, \quad \frac{\Delta T}{T_L} = \frac{\sqrt{\pi}}{4}S_\infty \\ \Delta\beta &= \left(\frac{2}{\sqrt{\pi}} - \frac{9\sqrt{\pi}}{16}\right)S_\infty \end{aligned}\right\} \qquad [51]$$

and, by means of the equation of state,

$$\frac{\Delta\rho}{\rho_e} = \left(\frac{2}{\sqrt{\pi}} + \frac{5\sqrt{\pi}}{16}\right)S_\infty \qquad [52]$$

Here, the small deviations from phase-equilibrium are defined by:

$$\left.\begin{aligned} \frac{p_e}{p_\infty} &= 1 + \Delta z_e, \quad \Delta T = T_L - T_\infty \\ \beta &= 1 + \Delta\beta, \quad \Delta\rho = \rho_e - \rho_\infty, \end{aligned}\right\} \qquad [53]$$

since we have in mind first of all the case of net evaporation. A linearized expression for the mass flux is then readily available, and may be conveniently stated in the form

$$\dot{m} = \rho_e\sqrt{\frac{RT_L}{2\pi}}\Bigg[\underbrace{\frac{\Delta\rho}{\rho_e} + \frac{1}{2}\frac{\Delta T}{T_L}}_{\sqrt{\pi}S_\infty} - \underbrace{\Delta\beta}_{0.1314S_\infty} + \underbrace{\Delta F^-}_{\sqrt{\pi}S_\infty}\Bigg] \qquad [54]$$

showing the relative importance of the various contributions:

(i) Hertz–Knudsen theory

$$\left(\frac{\Delta\rho}{\rho_e} + \frac{1}{2}\frac{\Delta T}{T_L}\right)$$

(ii) non-equilibrium backscattering ($\Delta\beta$)

(iii) bulk velocity effect (ΔF^-).

The non-equilibrium backscattering is thus seen to be relatively small under conditions of weak evaporation, whereas the bulk velocity effect from the external state is not. The numbers fitted into [54] then show that the popular linearized Hertz–Knudsen formula underestimates the mass flux by a factor of about 2. Writing the expression in terms of $\Delta\rho$ alone, we have, after the use of [51], [52] and [53]

$$\dot{m} = (\rho_e - \rho_\infty)\sqrt{\frac{RT_L}{2\pi}}\,\frac{32\pi}{32 + 5\pi} \simeq 2.107(\rho_e - \rho_\infty)\sqrt{\frac{RT_L}{2\pi}} \qquad [55]$$

This important correction to the classical Hertz–Knudsen formula is, for the most part, due to the account of the macroscopic bulk velocity in the external state, which results from the evaporation process itself.

Since, in many cases, the pressure rather than the density is the natural choice for matching the variable against the external flow field, we also give the formula in terms of pressure difference

$$\dot{m} = \rho_e\sqrt{\frac{RT_L}{2\pi}}\,\frac{\Delta p}{p_e}\,\frac{32\pi}{32 + 9\pi} \simeq 1.668\,\frac{p_e - p_\infty}{\sqrt{2\pi RT_L}} \qquad [56]$$

Similar mass flux formulae have been arrived at by several authors, for instance Pao (1971), Kogan & Makashev (1971) and Sone & Onishi (1978), and the numerical factors differ only slightly due to specific approximations made in the various methods. These formulae also apply for the case of net condensation onto the phase boundary, for which $p_\infty - p_e > 0$ and $\dot{m} < 0$. Hence evaporation

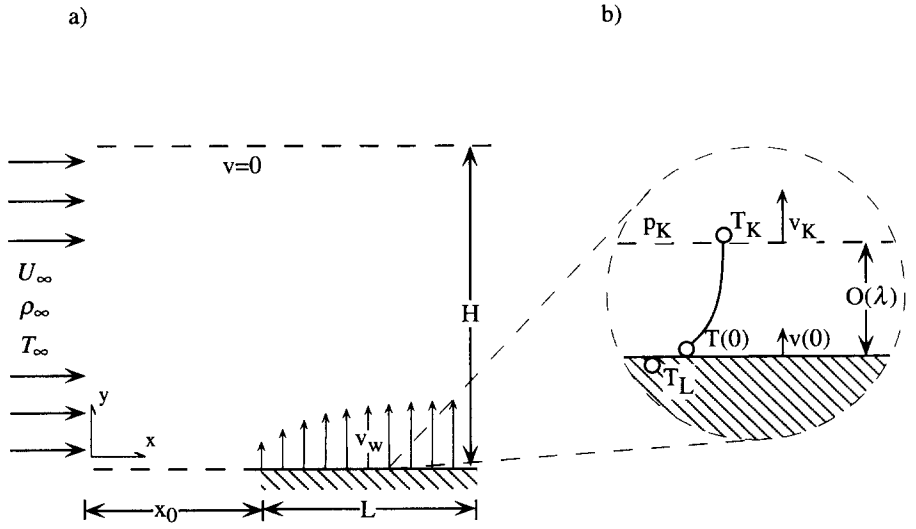

Figure 6. Definition sketch for evaporation into a shear flow. (a) External flow domain and (b) details from the Knudsen layer domain.

and condensation are antisymmetric phenomena in the linear regime, as long as only the Knudsen layers are considered.

3.4. Evaporation into a shear flow

As an example of the coupling that in general must be made between the Knudsen layer flow and an external flow field on a macroscopic scale, we now consider the situation indicated in figure 6. An initially uniform vapor-flow with parameters U_∞, p_∞ and T_∞ is approaching parallel to a flat surface of its own condensed phase, kept at rest and at temperature T_L. The condensed phase is furthermore confined to a thin flat plate with the leading edge at $x = x_0$, and with finite length L. We assume that the incoming vapor is saturated in its initial state and that $T_\infty < T_L$, and consequently that $p_\infty < p_{sat}(T_L) = p_e$. Hence, evaporation will occur at the interphase surface. It is also assumed that $(T_L - T_\infty)/T_L \ll 1$, $(p_e - p_\infty)/p_e \ll 1$, so that the linearized Knudsen layer results may be applied. In order not to confuse the notation, we use subscript k to indicate conditions at the outer edge of the Knudsen layer [figure 6(b)] reserving subscript ∞ for the undisturbed vapor-flow conditions at upstream infinity. The vapor flow field outside the Knudsen layer is described by standard two-dimensional Navier–Stokes equations with a k–ϵ model added to account for turbulence.

In the linear case the Knudsen layer folding length is 3/4 λ_e, and the thickness is therefore a few times this value. However, the smallest scale that occurs in the Navier–Stokes equations is of the order

$$\ell_{N.S} = \frac{\lambda_e}{S_k} \qquad [57]$$

and, since S_k is small in the sense ([50])

$$S_k \sim \frac{p_e - p_k}{p_e} \ll 1, \qquad [58]$$

in general we have

$$\ell_{N.S} \gg \lambda_e \qquad [59]$$

This is the basis for applying the formal matching condition

$$g\left(\frac{y}{\lambda_e} \to \infty\right) = G\left(\frac{y}{\ell_{N.S}} \to 0\right) \qquad [60]$$

between any two corresponding quantities g and G in the Knudsen-layer and Navier–Stokes solutions. This relates back to the fundamental issue of singular boundary layers for the Boltzmann equation in the limit of Kn→0, as mentioned in section 2.1. In particular we have, with reference to figure 6(a) and (b):

$$v_k = v_w, \quad T_k = T_w, \quad p_k = p_w \tag{61}$$

where subscript w denotes 'wall-values' for the Navier–Stokes variables and subscript k means 'infinity' in Knudsen layer variables. The true wall-values, as indicated by $v(0)$ and $T(0)$ in figure 6(b), occur only in the kinetic theory solution and are not further dealt with here.

From [61], [56] and [51] the particular boundary conditions that couple the Knudsen layer to the Navier–Stokes domain at $y = 0$, $x_0 \lesssim x \lesssim x_0 + L$, are:

$$v_w = \sqrt{2RT_L}\,\frac{4}{\sqrt{\pi}\beta_c}\,\frac{p_e - p_w}{p_e} \tag{62a}$$

$$T_w = T_L - \frac{T_L}{\beta_c}\,\frac{p_e - p_w}{p_e} \tag{62b}$$

with β_c as a new numerical factor

$$\beta_c = \frac{32 + 9\pi}{4\pi} \simeq 4.7965 \tag{63}$$

The wall-pressure in the Navier–Stokes solution is thus seen to be the matching parameter that determines the evaporation rate and the temperature at the exit of the Knudsen layer. Since the incoming vapor is in a saturated state, we also have, by the linearized Clapeyron equation,

$$T_\infty = T_L - \frac{T_L}{\beta_H}\,\frac{p_e - p_\infty}{p_L}, \tag{64}$$

where $\beta_H = \Delta H / RT_L$ is a substance parameter based on the latent heat of evaporation ΔH.

The Navier–Stokes equations were solved numerically on the physical domain shown in figure 6(a), using the TEACH-T code, where, in addition to the boundary conditions shown in the figure, a tangential no-slip condition at the interphase surface was applied, $u = 0$ for $y = 0$, $x_0 < x < x + L$, and a normal derivative condition $\partial u/\partial x = 0$ was imposed at the outlet, $x = x_0 + L$, $0 < y < H$. The slip boundary indicated at $y = H$ was introduced to limit the computational domain, and a distance $H \simeq 7L$ was found to be required for not causing local effects along the interphase surface.

The extent of the domain was then chosen as: $x_0 = 0.5$ m, $L = 0.55$ m, $H = 3.5$ m, and physical data were selected to represent water vapor close to atmospheric pressure: $T_L = 373.16$ K, $p_e = 1$ atm, with p_∞ in the range $0.97 - 0.998$ atm. A driving parameter for the problem is seen to be

$$\Delta\hat{p}_s = \frac{p_e - p_\infty}{p_e}, \tag{65}$$

and the constant latent heat parameter β_H takes the value 13.097, along with a gas constant $R = 461.96$ J/K/kg.

We considered incoming velocities U_∞ in the range 20–50 m/s, and we solved the discretized governing flow equations on rectangular grids ranging from 21 × 21 cells to 41 × 41 cells. The grids were contracted near the interphase surface and near the leading edge.

The TEACH-T code uses the SIMPLE algoritm (Patankar 1980), and start-values are required to initiate the iterations. We chose $U_{in} = U_\infty$, $p_{in} = p_\infty$ and $T_{in} = T_\infty$ as initial values, from which values for the boundary conditions v_w and T_w were obtained by [62a] and [62b] with $p_w = p_\infty$. This would then start an iteration on the parameter $(p_e - p_w)/p_e$ in these equations, such that

$$\left(\frac{p_e - p_w}{p_e}\right)_1 = \frac{p_e - p_\infty}{p_e} = \Delta\hat{p}_s,$$

and a converged solution would normally be obtained after 300–400 iterations in the system. Some typical results for a case with $U_\infty = 20$ m/s and $\Delta p_s = 2.1 \times 10^{-3}$ are shown in figure 7 [from

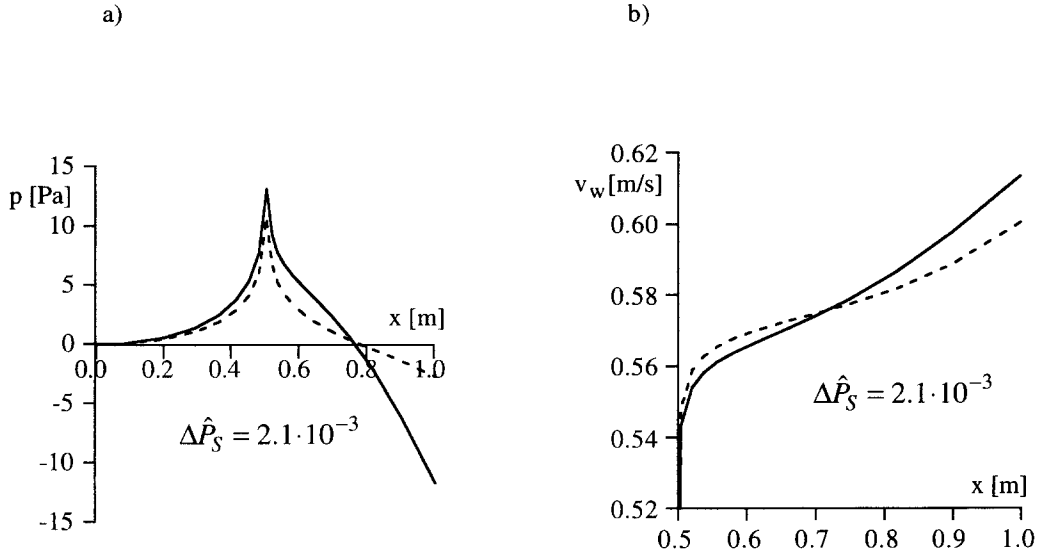

Figure 7. Results for evaporation into a shear flow in the case: $U_\infty = 20$ m/s, $\mathrm{Re} = 5.2 \times 10^5$, $\Delta\hat{p}_s = 2.1 \times 10^{-3}$. (a) Pressure along baseline/surface and (b) evaporation velocity normal to surface.

Stinessen (1988)]. The dotted lines are for laminar flow, whereas the solid lines represent turbulent flow, in both cases for a Reynolds number of 5.21×10^5, based on the plate length. The turbulence intensity was then set low, typically 10^{-5}, in the incoming flow, but developed very quickly as the leading edge of the plate and the cross-flow region was approached.

We see that the pressure at $y = 0$ is almost symmetric around the leading edge in the laminar case, but that generation of turbulence distorts this picture somewhat. At the downstream part of the plate the two solutions develop rather differently. However, in both cases we see qualitatively similar trends, and these Navier–Stokes predicted pressures are both very different from the constant value that is assumed in classical boundary layer theory for shear flow along a non-reactive surface. This is clearly due to the fact that the injection velocities considered here are much larger than typical lateral boundary layer velocities, $v_{\mathrm{B.L}}$, so that a boundary layer would be blown off from the surface immediately after the injection is introduced. We have in the present case:

$$v_w \simeq \sqrt{2RT_L}\frac{p_e - p_\infty}{p_e} \simeq 1 \text{ m/s}$$

$$v_{\mathrm{B.L}} \simeq U_\infty/\sqrt{\mathrm{Re}} \simeq 10^{-2} \simeq 10^{-1} \text{ m/s},$$

and in general, typically $v_w \gg v_{\mathrm{B.L}}$. The pressure field is hence, in effect, computed from an elliptic Poisson type of equation with an upstream influence length of the same order of magnitude as the geometrical scale of the problem, as is normally the case for full Navier–Stokes solutions.

The pressure at the wall is generally higher than p_∞ at the upstream part of the surface and lower than p_∞ downstream. In the case shown in figure 7(a) the shift occurs at about $x = 0.75$ m, which is half-way down the evaporating surface. At this point the injection velocity and the mass flux are predicted by the value p_∞ for p_w in the expression [62], which, from figure 7(b), corresponds to $v_w \simeq 0.58$ m/s. This corresponds, furthermore, to the first iteration in the solution, and would be the natural estimate to make for the average injection velocity, in the lack of local resolution of the problem.

The increase in injection velocity as we move downstream along the surface [figure 7(b)] follows directly from the falling trend of p_w. But this is all conditional by the thermostat assumption for the liquid phase; $T_L = \text{const.}$, which leads to $p_e = p_{\mathrm{sat}}(T_L) = \text{const.}$, too. For different thermal conditions in the dense phase, the results would be different, but the matching principle and this method of solution would still apply.

In principle, the boundary conditions [62] could have been expressed in terms of temperature $T_L - T_w$ instead of pressure $p_e - p_w$, and the coupling could have been attempted in the energy

equation instead of in the momentum equation of the Navier–Stokes system. However, the temperature field can be determined only after the velocity and pressure fields are known, so therefore the velocity and pressure would have to be solved for initially in any case, which requires the original version [62] as input, with pressure as the primary variable.

Finally, it should be remarked that the present approach assumes the normal continuum flow conditions [7] and [19] to be valid. Should they not be, so that $M/\sqrt{Re}$ is not a small quantity, as would occur in high-speed or low-density cases, the Knudsen layer may no longer be simply separated from the rest of the flow field, and the Boltzmann equation may have to be applied to a global scale of the problem.

3.5. Thermodynamic aspects of the vapor

Since the complete state of the vapor flow in the Knudsen layer—including its external edge—is determined from the Boltzmann equation alone, there is no reason to assume that such states will, in general, correspond to saturation. This may simply be demonstrated from the linearized results, with immediate extensions to the general non-linear case.

The pressure–temperature relation across the Knudsen layer is conveniently represented in [62], which we rewrite as

$$\Delta\hat{p} = \beta_c \Delta\hat{T}, \qquad [66]$$

in which Δp and ΔT are the normalized differences $(p_e - p_k)/p_e$ and $(T_L - T_k)/T_L$, respectively. On the other hand, if the state (T_k, p_e) at the edge of the Knudsen layer is replaced by a saturated state (T_{sat}, p_{sat}), we obtain from the linearized Clapeyron equation

$$\Delta\hat{p}_{sat} = \beta_H \Delta\hat{T}_{sat} \qquad [67]$$

where $\beta_H = \Delta H/RT_L$ is the normalized latent heat parameter. By comparison of the two expressions above, we find that the superheat ΔT_s is given by

$$\Delta T_s = T_k - T_{sat} = (\beta_c - \beta_H)\frac{\Delta T}{\beta_H}, \qquad [68]$$

where again $\Delta T = T_L - T_k$. Now, β_c is a constant parameter in the linear evaporation regime, and according to [63] it has the value 4.7965. Then, for latent heat parameters below this value the vapor is superheated, whereas substances with latent heat parameters above this value will be supercooled, or supersaturated when they leave the Knudsen layer, as simply expressed by [68]. According to Troutons rule, most common substances will have β_H values of the order of 10, so therefore, in most cases, supersaturation must be expected to occur. In particular, for water vapor at $T_L = 373.16$ K, the value was found to be $\beta_H = 13.097$. The boundary values applied at the surface in the shear flow problem of the previous section therefore represent a highly supersaturated state, and the possibility of homogeneous recondensation and formation of mist should be taken into account in such cases.

The situation in the general non-linear case is not much different. The parameter β_c will depend upon the flow conditions and will be given by the expression

$$\beta_c = \frac{\ln(p_e/p_k)}{1 - T_k/T_L}; \qquad [69]$$

otherwise [68] remains valid. The parameter takes values that are rather close to the one for the linear case, but the temperature difference $\Delta T = T_L - T_k$ is much larger and so becomes ΔT_s.

A final and interesting observation may be made with reference to the case $S_\infty = 0.5$ in figure 3 as discussed in section 3.1. Evaluating the parameter β_c according to [69] at the edge of the Knudsen layer gives the value 4.79, whereas at the interphase boundary with $T(0)$ and $p(0) = \rho(0)RT(0)$ we get 3.75. The absolute value of the difference $\beta_c - \beta_H$ will therefore be larger in the latter position, if water vapor with $\beta_H \simeq 13$ is again considered. The temperature difference in the expression corresponding to [68] will, however, be smaller, since $T_L - T(0) \lesssim T_L - T_k$, and when the figures are worked out, we obtain $\Delta T_s \simeq -0.126\, T_L$ at infinity, and $\Delta T_s \simeq 0.107\, T_L$ at the surface. This result shows that the supersaturation for a large part is caused by the actual phase change itself;

i.e. from $T = T_L$ to $T = T(0)$ across the interphase surface, and that the effect is further slightly enhanced as the vapor expands through the Knudsen layer.

3.6. *Effect of non-unity evaporation–condensation coefficient*

So far all the results have been derived under the assumption that the evaporation–condensation coefficient a_w in [10] has been unity, such that the reflection mode f_r in that equation and in figure 1 has been absent. Although experimental information on the coefficient a_w in interphasial processes is scarce, it is known that its value may vary considerably below 1, depending upon the actual substance considered and upon the surface conditions. This view is further substantiated by recent molecular dynamics simulations of the phase transition (Matsumoto 1995) from which values for a_w down to 10^{-3} are extracted under certain realistic circumstances. Therefore, it is of considerable interest from a practical point of view to incorporate the effect of non-unity a_w in the theory of evaporation–condensation phenomena.

Assuming that the fraction $(1 - a_w)$ of the impinging molecules is reflected from the interface according to a Maxwellian distribution f_r at the surface temperature T_L, we have the flux condition

$$\int_{\xi_y<0} \xi_y f_r \underline{\mathrm{d}\xi} = (1 - a_w) \int_{\xi_y>0} |\xi_y f(0,\xi)| \underline{\mathrm{d}\xi} \qquad [70]$$

in which $f(0, \xi)$ for $\xi_y < 0$ is inserted from [22]. For the related density this gives

$$\rho_r = (1 - a_w)\rho_\infty \sqrt{\frac{T_\infty}{T_L}}\, \beta F^-(S_\infty) \qquad [71]$$

Thus the slightly more general boundary condition is obtained by replacing the density ρ_e by the new expression

$$\rho_e \to a_w \rho_e + (1 - a_w)\rho_\infty \sqrt{\frac{T_\infty}{T_L}}\, \beta F^-(S_\infty) \qquad [72]$$

which allows the original results to be transformed to the more general case in a simple way, as shown for instance by Kogan & Makashev (1971) and Sone & Sugimoto (1993). Here we give the final results only for the linear case of weak evaporation and condensation, for which the mass flux formula [55] transforms into

$$\dot{m} = (\rho_e - \rho_\infty)\sqrt{\frac{RT_L}{2\pi}}\, \frac{a_w}{1 - \left(\frac{27}{32} - \frac{1}{\pi}\right)a_w} \qquad [73]$$

From this expression we see that the mass flux decreases faster than linearly with decreasing a_w, in particular in the range of a_w that is not much below unity. For small values of a_w the variation is essentially linear, since the numerical factor in the denominator of [73] has the value 0.5254. This latter figure should be compared to 0.535 from Kogan & Makashev (1971) and 0.5246 from Sone & Onishi (1978).

Also the thermodynamic state of the vapor is affected by the evaporation–condensation coefficient. Instead of [68], the superheat ΔT_s is now given by the expression

$$\Delta T_s = T_k - T_{sat} = \left(\beta_c + 8\frac{1 - a_w}{a_w} - \beta_H\right)\frac{\Delta T}{\beta_H} \qquad [74]$$

where, again, $\beta_c = 4.7965$, $\Delta T = T_L - T_k$ and $\beta_H = \Delta H / RT_L$ is the latent heat parameter.

For a case of $a_w = 0.5$, the limit between superheat and supercooling is shifted to $\beta_H = 12.7965$ (from $\beta_H = 4.7965$), closely corresponding to the value of β_H for water at 373 K. Substances with a latent-heat parameter above this value will then give supersaturated vapor, whereas substances

with values below it will be superheated. As is evident from [74], the actual limit is very sensitive to the value taken by the coefficient a_w.

4. CONCLUDING REMARKS

We have shown that a molecular description is required to capture the basic fluid-flow and thermodynamics aspects of interphasial processes in single-component liquid–vapor or solid–vapor systems. A quantitative analysis has been performed based on a four-moment solution of the Boltzmann equation, which to the best of our knowledge, is still the only analytic solution available for arbitrarily strong evaporation. Several specific points have been made, such as:

(i) a consistent definition of the external vapor state and its coupling to the dense-phase temperature T_L in terms of one single control parameter, the pressure-ratio p_e/p_∞, where $p_e = p_{sat}(T_L)$,
(ii) the existence of a limiting upper value for this parameter, $(p_e/p_\infty)_{cr} \simeq 4.81$, corresponding to sonic velocity of the vapor flow away from the interphase surface,
(iii) an interpretation and assessment of the Hertz–Knudsen and Schrage mass transfer formulae, and the need for a proper definition of the external vapor state in order for these formulae to work well,
(iv) the role of the pressure as a prime variable in the matching between the molecular and continuum flow regimes in a global problem treatment, with shear-flow outside of the normal-flow evaporation–condensation layer, and
(v) the strong tendency for common substances (in the sense of Trouton) to become supersaturated in evaporation, for unity or, near unity, evaporation–condensation coefficient.

Our main findings agree well, also at the quantitative level, with results from more accurate numerical resolutions of the detailed Boltzmann equation, and with Monte Carlo simulations, in the whole flow regime of evaporation. This indicates that the kinetic theory approach has, in general, led to converged results for evaporation, and, at least in the linear case, also for condensation.

It appears that the most ambiguous element in the theory lies in the gas kinetic boundary conditions, relating to such elements as evaporation and condensation coefficients for surfaces that are active in the phase-transfer process. Values for such coefficients must be obtained experimentally, or by molecular dynamics considerations in the dense phase, and they may indeed turn out to depend upon the intensity of the process. This is to be suspected on the background of the significant and rate-dependent temperature jump across the interphase surface that is predicted in the present study.

REFERENCES

Anisimov, S. I. 1968 Metal evaporation by laser radiation. *J. Eksperim. Teor. Fisika* **54,** 339–342.

Aoki, K. & Cercignani, C. 1983 Evaporation and condensation on two parallel plates at finite Reynolds numbers. *Phys. Fluids* **26,** 1163–1168

Aoki, K., Nishino, K., Sone, Y. & Sugimoto, H. 1991 Numerical analysis of steady flows of gas condensing on or evaporating from its plane condensed phase on the basis of kinetic theory. *Phys. Fluids A* **3,** 2260–2275.

Aoki, K., Sone, Y. & Yamada, T. 1990 Numerical analysis of gas flows condensing on its plane condensed phase on the basis of kinetic theory. *Phys. Fluids A* **2,** 1867–1878.

Cercignani, C. 1981 Strong evaporation of a polyatomic gas. In *Rarefied Gas Dynamics* (Edited by Fisher, S.), Vol. 74, pp. 305–320. Prog. Astronaut. Aeronat. AIAA, New York.

Chapman, S. & Cowling, T. G. 1952 *The Mathematical Theory of Nonuniform Gases*. Cambridge University Press.

Cipolla, J.W., Lang, J.H. & Loyalka, S.K. 1973 Kinetic theory of evaporation and condensation. In *Rarefied Gas Dynamics* (Edited by Karamcheti, K.), pp. 179–188. Academic Press, New York.

Crifo, J. F. 1986 Comets as large dirty snowballs subliming in interplanetary space. In *Rarefied Gas Dynamics* (Edited by Boffi, V. & Cercignani, C.), pp. 229–250. Teubner, Stuttgart.

Edwards, R. H. & Collins, R. L. 1969 Evaporation from a spherical source into a vacuum. In *Rarefied Gas Dynamics* (Edited by Trilling, L. & Wachmann, H. Y.), pp. 1489–1496. Academic Press, New York.

Ferron, J. 1986 Four-moment model of one-dimensional multicomponent distillation at high vacuum. In *Rarefied Gas Dynamics* (Edited by Boffi, V. & Cercignani, C.), pp. 301–312. Teubner, Stuttgart.

Frezzotti, A. 1986 Kinetic theory study of the strong evaporation in a binary mixture. In *Rarefied Gas Dynamics* (Edited by Boffi, V. & Cercignani, C.), pp. 313–322. Teubner, Stuttgart.

Frezzotti, A. 1991 Numerical investigation of the strong evaporation of a polyatomic gas. In *Rarefied Gas Dynamics* (Edited by Beylich, A.), pp. 1243–1250. VCH, Weinheim.

Gajewski, P., Kulicki, A. Wisniewski, A. & Zgorelski, M. 1974 Kinetic theory approach to the vapor-phase phenomena in a non-equilibrium condensation process. *Phys. Fluids* **17,** 321–327.

Hertz, H. 1882 Ueber die Verdunstung der Flüssigkeiten, insbesondere des Quecksilbers, im luftleeren Raume. *Ann. Phys. Chem.* **17,** 177–200.

Knudsen, M. 1915 Die Maximale Verdampfungsgeschwindigkeit des Quecksilbers. *Ann. Phys. Chem.* **47,** 697–708.

Kogan, M. N. 1992 Kinetic theory in aerothermodynamics. *Prog. Aerospace Sci.* **29,** 271–354.

Kogan, M. N. & Abramov, A. A. 1991 Direct simulation of the strong evaporation and condensation problem. In *Rarefied Gas Dynamics* (Edited by Beylich, A.), pp. 1251–1257. VCH, Weinheim.

Kogan, M. N. & Makashev, N. K. 1971 Knudsen layer in the theory of heterogeneous reactions. *Akad. Nauk. SSSR, Mech. Zhidk Gaza* **6,** 3–11 (in Russian); also *Fluid Dynam.* **6,** 913–921.

Kryukov, A. P. 1991 Strong subsonic and supersonic condensation on a plane surface. In *Rarefied Gas Dynamics* (Edited by Beylich A.), pp. 1278–1284. VCH, Weinheim.

Kucherov, R. Ya. & Rikenglas, L. E. 1960 On hydrodynamic boundary conditions with evaporation of a solid absorbing radiant energy. *Soviet Phys. JETP* **37,** 10–11.

Luikov, A. V., Perleman, T. L. & Anisimov, S. I. 1971 Evaporation of a solid into vacuum. *Int. J. Heat Mass Transfer* **14,** 177–183.

Mager, R., Adomeit, G. & Wortberg, G. 1989 Theoretical and experimental investigation of strong evaporation of solids. In *Rarefied Gas Dynamics* (Edited by Muntz, E. P., Weaver, D. P. & Campbell, D. H.), pp. 460–469. AIAA, Washington, DC.

Matsumoto, M. 1995 Molecular dynamics of evaporation and condensation. *Proc. 2nd. Int. Conf. Multiphase Flow '95*, Supplement, p. 69 (Abstract only).

Murakami, M. & Oshima, K. 1974 Kinetic approach to the transient evaporation and condensation problem. In *Rarefied Gas Dynamics* (Edited by Becker, M. & Fiebig, M.), Vol. 1, p. F6. DFVLR Press, Portz-Wahn.

Nanbu, K. 1986 Rarefied gas dynamics problems on fabrication process of semiconductor films. In *Rarefied Gas Dynamics* (Edited by Boffi, V. & Cercignani, C.), pp. 410–419. Teubner, Stuttgart.

Onishi, Y. 1986 The spherical droplet problem of evaporation and condensation in vapor–gas mixture. *J. Fluid Mech.* **163,** 171–194.

Patankar, S. 1980 *Numerical Heat Transfer and Fluid Flow*. Hemisphere, New York.

Patton, A.J. & Springer, G.S. 1969 A kinetic theory description of liquid vapor phase change. In *Rarefied Gas Dynamics* (Edited by Trilling, L. & Wachman, H.Y.), pp. 1497–1504. Academic Press, New York.

Schrage, R. W. 1953 *A Theoretical Study of Interphase Mass Transfer*. Columbia University Press, New York.

Shankar, P. N. & Marble, F. E. 1971 Kinetic theory of transient condensation and evaporation at a plane surface. *Phys. Fluids* **14,** 510–516.

Sibold, D. & Urbassek, M. 1993 Monte Carlo study of Knudsen layers in evaporation from elemental and binary media. *Phys. Fluids* **A5,** 243–255.

Sone, Y. & Onishi, Y. 1978 Kinetic theory of evaporation and condensation—hydrodynamic equations and slip boundary conditions. *J. Phys. Soc. Jpn* **44,** 1981–1994.

Sone, Y., Aoki, K., Sugimoto, H. & Yamada, T. 1990 Steady evaporation and condensation on a plane condensed phase. *Phys. Fluids* **A2** (10), 1867–1878.

Sone, Y. & Sugimoto, H. 1993 Kinetic theory analysis of steady evaporating flows from a spherical condensed phase into vacuum. *Phys. Fluids* **A5,** 1491–1511.

Stinessen, M. 1988 Injection into a turbulent shear flow. SINTEF, Div. Appl. Phys. Report STF 19A88003, Trondheim (in Norwegian).

Sugimoto, H. & Sone, Y. 1992 Numerical analysis of steady flow of a gas evaporating from its cylindrical condensed phase on the basis of kinetic theory. *Phys. Fluids A* **4,** 419–440.

Vincenti, W. G. & Kruger, C. H. 1965 *Introduction to Physical Gas Dynamics*, pp. 361–368. Wiley, New York.

Yen, S. M. 1973 Numerical solutions of non-linear kinetic equations for a one-dimensional evaporation–condensation problem. *Computers Fluids* **1,** 367–377.

Ytrehus, T. 1977 Theory and experiments on gas kinetics in evaporation. In *Rarefied Gas Dynamics* (Edited by Potter, L.), Vol. 51 of Prog. Aeronaut., pp. 1197–1212. AIAA, New York.

Ytrehus, T. & Aukrust, T. 1986 Mott–Smith solution for weak condensation. In *Rarefied Gas Dynamics* (Edited by Boffi, V. & Cercignani, C.), pp. 271–280. Teubner, Stuttgart.

Ytrehus, T., Smolderen, J.J. & Wendt, J.F. 1977 Mixing of thermal molecular jets produced from Knudsen effusion. *Entropic* **42,** 33–39.

Ytrehus, T. & Stinessen, M. 1991 Strong evaporation in the presence of inert solid particles. In *Rarefied Gas Dynamics* (Edited by Beylich, A.), pp. 1235–1242. VCH, Weinheim.